TURBULENT CHARACTERISTICS ANALYSIS OF NEAR-CYLINDER WAKE BASED ON DATA-DRIVEN METHODS

Yafei Zhong
Research Institute of Aero-Engine, Beihang
University, Beijing 102206, China

Hongwei Ma
School of Energy and Power Engineering,
Beihang University, Beijing 102206, China
Research Institute of Aero-Engine, Beihang
University, Beijing 102206, China

ABSTRACT

The cylindrical probe strut will block the compressor's internal flow field and deteriorate its performance. It is significant to cognize the turbulence characteristics of the cylindrical strut wake for a deep understanding of the interference mechanism of the strut wake on the compressor. Particle image velocimetry was used in a water tunnel to investigate the turbulent characteristics of the near-cylinder wake at Reynolds number Re = 4000. The results reveal that the high-frequency structures are symmetrically distributed throughout the near-cylinder wake, and the wake is absolute instability during the Karman-vortex formation. For the comparative evaluation of detecting the dominant flow structures, three data-driven methods were utilized: Proper Orthogonal Decomposition (POD), Dynamic Mode Decomposition (DMD) and multi-scale Proper Orthogonal Decomposition (mPOD). The results demonstrate that DMD can extract distinctive features in the cylinder wake corresponding to the main frequency, harmonics, and Kelvin-Helmholtz (K-H) instability. POD is more successful than DMD at removing flow field noise, although it cannot purify the spectrum. As a result, identifying high-frequency harmonics and the K-H vortex is challenging. mPOD has both benefits, as well as strong noise filtering and high-frequency structure detection. mPOD retrieved the phase-locked signal of the wake. The phase-averaging approach reveals that during the formation of the Karman vortex, turbulent kinetic energy is mostly produced in the shear convection between the Karman vortex and the mainstream and eventually travels to the vortex core area and dissipates there. Then, mPOD established a relationship between the flow structures and turbulent energy dissipation, with turbulent energy dissipation attributable to the formation of large-scale Karman vortex, free shear layer convection and K-H vortex shedding.

INTRODUCTION

The pneumatic probe, being one of the most mature measurement methods, is frequently employed in the compressor measurement process to get the internal flow parameters of the compressor. The probe strut is cylindrical, and the flow around it is at subcritical Reynolds numbers. The turbulent wake features complicated flow structures like the Karman vortex, the K-H vortex [1–3], the dissipative vortex, etc. The strut's low-speed wake will block the blade channel, increasing the attack angle and making it easier for the compressor to enter instability. The mixing of the strut wake and the mainstream causes a substantial quantity of small-scale turbulent dissipation, which increases the compressor's energy loss and degrades its performance [4–8]. Furthermore, the periodic flow structure interacts with the blades, causing irregular vibration of the blade. Figure 1 depicts the mixing diagram of the strut wake and the compressor's mainstream. As a result, it is critical to clarify the turbulence characteristics of the cylindrical strut wake in order to comprehend the interference mechanism of the strut wake on the compressor and to conduct wake control research.
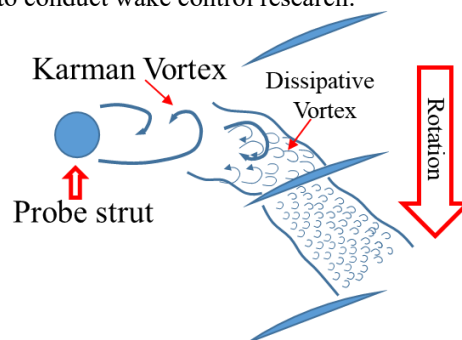

Figure 1 Mixing of strut wake and compressor main stream principle diagram

Relevant studies have revealed that the wake of a circular cylinder in the subcritical zone has a strong two-dimensionality, and because the probe is relatively close to the compressor inlet, the wake near the cylinder is required to be measured. Hotwire, LDV, and PIV are some instances of conventional velocity field measurements. In comparison to hotwire and LDV, PIV technology, which has the benefit of flow field surface measuring, has matured significantly. As a result, the two-dimensional wake near the cylinder is measured using PIV technology in this research. For investigating the features of cylinder wakes, the data-driven method breaks down the original flow field into numerous modes, and the exacted modes provide energy or frequency information, allowing for the identification of unique flow structures, noise filtering, and mechanism analysis [9–12]. Data-driven approaches have been frequently employed in PIV data analysis of bluff body wakes due to their capacity to do spatiotemporal analysis. POD [12–20] and DMD [21–30] are the two most extensively utilized data-driven approaches at the moment.

POD employs eigenvalue decomposition to generate a sequence of orthogonal bases with energy optimization and then sorts the eigenvalues to find the modes with a lot of energy. Due to their high energy, the low-order mode often corresponds to the large-scale flow structure, whereas the high-order mode typically relates to the small-scale turbulence structure [31]. Zheng et al. performed PIV tests on the wake of a porous cylinder and used the POD method to examine the wake's unsteady features [13]. The results demonstrate that the first and second modes relate to alternating vortex shedding, whereas the third and fourth modes correlate to symmetrical vortex shedding. Liu et al. employed the first two POD modes to reconstruct the phase-averaged flow field of the grooved cylinder wake [32]. They discovered that the major flow structure of the grooved cylinder wake is the shear layer's symmetrical vortex, which considerably decreases the cylinder's drag. Because low-order modes carry the majority of the information in the cylindrical wake, several low-order modes could be employed to reconstruct the flow field, filter out high-order noise interference, and extract the flow field's crucial data.

POD can decouple flow field space but cannot purify the time spectrum. According to the preceding discussion, the flow pattern in the cylinder's wake is complicated, and the distinctive structure is often linked with a certain frequency. For example, the Karman vortex shedding frequency, its harmonics, the main frequency of the K-H instability, and so on. As a result, obtaining the flow structure at a single frequency is critical for analyzing the properties of the cylinder wake. DMD can realize frequency purification, which provides a method for solving the above problems. The relevant theory may be found in Schmid's study results [23]. Tissot et al. employed DMD to investigate the dynamic properties of the smooth circular cylinder wake flow field via flow field reconstruction [33]. Zhang et al. utilized DMD to evaluate the flow characteristics of a near-wall cylinder wake at a low Reynolds number, obtaining the dominant frequency and the frequency harmonic mode with a gap [21]. Higham et al. investigated the wake dynamics of porous square cylinders using a combination of DMD and POD, analyzing the dominant frequency of wakes and flow structure under different porous distribution structures [34].

While DMD can perform frequency purification, it cannot obtain orthogonal energy modes. Mendez et al. proposed the multi-scale POD method (mPOD) based on the above modal extraction method to compromise energy optimization and frequency purification [35]. This method combines multi-resolution analysis (MRA) to apply the filter bank to the POD mode. POD and mPOD were used to compare and evaluate the characteristics of jet impinging on a flat plate. When compared with POD, mPOD achieves identification of wall separation vortex structure and jet vortex structure. Then, Mendez et al. performed mPOD on the PIV data of the flow around the cylinder in the transition state and discovered that, when compared with POD, mPOD has the advantage of frequency purification, particularly the dominant feature extraction of the cylinder in the transition state. Additionally, it was discovered that it has good convergence when compared with the DMD [36].

Some research on the turbulent characteristics of the cylinder wake uses the phase-averaging approach to investigate the characteristics of turbulence production, transport, and dissipation. Perrin et al. employed PIV in conjunction with phase averaging to investigate the turbulent kinetic energy of a smooth cylinder wake as well as the distribution of the turbulent kinetic energy production rate. They discovered that turbulent kinetic energy tends to go from the shear layer to the wake center line[37]. Chen et al. obtained velocity information of the subcritical cylindrical wake using a hot wire probe with four X-shaped probes and discovered that turbulence energy dissipation occurred mostly in the Karman vortex core[38]. Jiang et al. used DNS in conjunction with the phase-averaging approach to investigate the energy dissipation characteristics of the cylinder wake. It was discovered that the turbulent kinetic energy in the wake vortex's shedding zone was primarily created at the saddle point, carried to the Karman vortex core, and eventually dissipated in the vortex core region[39].

However, the wake is absolute instability, and the disturbance growth rate is greater than 0 in the near-cylinder wake zone, where the Karman vortex is gradually forming. After the Karman vortex shedding, the wake eventually stabilizes when the disturbance growth rate of the wake is less than 0. As a result, the near-cylinder wake's turbulence properties are distinct from those of the Karman vortex shedding. However, the turbulence characteristics of the near-cylinder wake are not fully described in the aforementioned literature. Furthermore, the quantitative investigation of wake turbulence dissipation control may be supported by the decomposition of

turbulent energy dissipation using the data-driven method and establishing the link between flow structure and turbulent energy dissipation. However, relevant research content has yet to be discovered in the literature.

To address the shortcomings of the preceding study, PIV experimental research on the turbulent characteristics of the near-cylinder wake was conducted in a water tunnel. The test scheme, PIV measurement system, and measurement accuracy analysis were all introduced in Section 2.1. In Section 2.2, FFT was used to study the time-frequency characteristics of the cylinder wake, and the OS equation was solved to assess the wake's instability. Section 2.3 compares the potential of several data-driven approaches (POD, DMD, mPOD) to detect typical flow structures corresponding to the main frequency, main-frequency harmonics, and Kelvin-Helmholtz (K-H) instability in the wake. The phase-averaging signal of the wake is generated by the low-order reconstructed flow field using mPOD, and the turbulence properties of the near-cylinder wake are characterized by the phase averaging method. The convergence of the mPOD in turbulent energy dissipation is confirmed in section 2.4, the energy dissipation is decomposed, and the association between the cylinder wake's flow structure and turbulence dissipation is established. Finally, the conclusions are summarized in Section 3.

RESULTS AND DISCUSSION

The phase-averaging contours are shown in Figure 2 (a)-(d). The figure shows that, due to the influence of the flow field's shear stress and velocity deformation, the production rate of the wake turbulent is primarily distributed in the wake vortex's shear convection zone, and the saddle point during the formation of the Karman vortex. At the same time, the turbulent kinetic energy contour is comparable to the production rate, but approaches the vortex core. The energy dissipation of turbulence is mostly dispersed in the center of the Karman vortex, which is comparable to vorticity. This demonstrates that turbulence in the near-cylinder wake region is primarily accompanied by the formation of large-scale Karman vortex, which transfers to the core area of the Karman vortex and subsequently dissipates there.

All modes are categorised according to the frequency bands separated using DMD by obtaining the characteristic frequency of mPOD mode coefficients. The average dissipation contours are obtained by reconstructing the first 15 modes in each frequency band, as illustrated in Figure 2 (e) - (j). The average dissipation of the reconstructed flow field gradually spreads to the wake boundary near the cylinder as the frequency increases. The main reason is that as frequency increases, the reconstructed vortex structure gradually shifts from the large-scale Karman Vortex to the small-size K-H vortex; because wake dissipation is mostly dispersed in the vortex core, energy dissipation approaches the convection zone at the wake's edge with increasing frequency. The energy dissipation of the modes in FB1-FB2 is attributed to the formation of the Karman vortex, according to the reconstructed flow field contours in each frequency band. The energy dissipation of the modes in FB3-FB4 is caused by free shear convection, whereas the K-H vortex causes the energy dissipation in FB5-FB6.
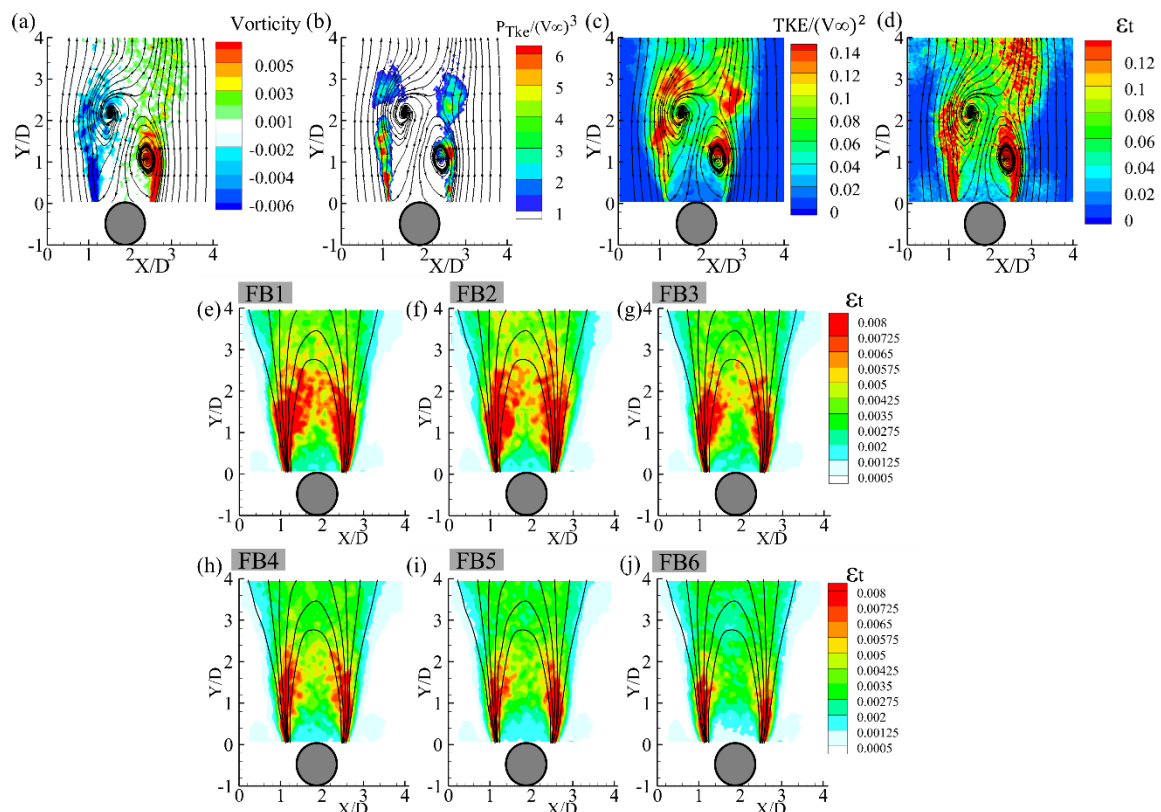
Figure 2. **Phase-averaging contours: (a) vorticity; (b)turbulence production rate; (c) turbulence kinetic energy; (d) turbulence energy dissipation rate, and the energy dissipation contours of the mPOD modes in different frequency bands (e) FB1; (f) FB2; (g) FB3; (h) FB4; (i) FB5; (j) FB6**

REFERENCES

[1] J.F. Derakhshandeh, M.M. Alam, A review of bluff body wakes, Ocean Eng. 182 (2019) 475–488. https://doi.org/10.1016/j.oceaneng.2019.04.093.

[2] D.E. Aljure, O. Lehmkhul, I. Rodríguez, A. Oliva, Three dimensionality in the wake of the flow around a circular cylinder at Reynolds number 5000, Comput. Fluids. 147 (2017) 102–118. https://doi.org/10.1016/j.compfluid.2017.02.004.

[3] R. Perrin, M. Braza, E. Cid, S. Cazin, F. Thiele, J. Borée, Time Resolved Stereoscopic PIV measurements in the near wake of a circular cylinder at high Reynolds number, (2008).

[4] J. Lepicovsky, Effects of a Rotating Aerodynamic Probe on the Flow Field of a Compressor Rotor, (2008).

[5] A. Islam, H. Ma, Numerical study of probe parameters on performance of a transonic axial compressor, PLOS ONE. 16 (2021) e0245711. https://doi.org/10.1371/journal.pone.0245711.

[6] H. Ma, S. Li, W. Wei, Effects of probe support on the flow field of a low-speed axial compressor, J. Therm. Sci. 23 (2014) 120–126. https://doi.org/10.1007/s11630-014-0685-7.

[7] H. Ma, S. Li, W. Wei, Effects of Probe Support on the Stall Characteristics of a Low-Speed Axial Compressor, J. Therm. Sci. 25 (2016) 43–49. https://doi.org/10.1007/s11630-016-0832-4.

[8] Y. Zhong, H. Ma, Y. Yang, Effects of Probe Stem Surface Suction on the Aerodynamic Performance of a Compressor, in: Vol. 2A Turbomach. — Axial Flow Fan Compress. Aerodyn., American Society of Mechanical Engineers, Virtual, Online, 2021: p. V02AT31A024. https://doi.org/10.1115/GT2021-59047.

[9] L. Shi, _H_ Ma, X. Yu, POD analysis of the unsteady behavior of blade wake under the influence of laminar separation vortex shedding in a compressor cascade, Aerosp. Sci. Technol. 105 (2020) 106056. https://doi.org/10.1016/j.ast.2020.106056.

[10] R. Gurka, A. Liberzon, G. Hetsroni, POD of vorticity fields: A method for spatial characterization of coherent structures, Int. J. Heat Fluid Flow. 27 (2006) 416–423. https://doi.org/10.1016/j.ijheatfluidflow.2006.01.001.

[11] M. Ben Chiekh, M. Michard, M.S. Guellouz, J.C. Béra, POD analysis of momentumless trailing edge wake using synthetic jet actuation, Exp. Therm. Fluid Sci. 46 (2013) 89–102. https://doi.org/10.1016/j.expthermflusci.2012.11.024.

[12] M. Raiola, S. Discetti, A. Ianiro, On PIV random error minimization with optimal POD-based low-order reconstruction, Exp. Fluids. 56 (2015) 75. https://doi.org/10.1007/s00348-015-1940-8.

[13] C. Xia, Z. Wei, H. Yuan, Q. Li, Z. Yang, POD analysis of the wake behind a circular cylinder coated with porous media, J. Vis. 21 (2018) 965–985. https://doi.org/10.1007/s12650-018-0511-5.

[14] Y. Zheng, A. Rinoshika, S. Fujimoto, Triangle Cylinder Wake Analysis Based on Wavelet and POD Techniques, Procedia Eng. 126 (2015) 108–112. https://doi.org/10.1016/j.proeng.2015.11.188.

[15] S. Yarusevych, M. Kotsonis, Effect of Local DBD Plasma Actuation on Transition in a Laminar Separation Bubble, Flow Turbul. Combust. 98 (2017) 195–216. https://doi.org/10.1007/s10494-016-9738-1.

[16] R. Perrin, M. Braza, E. Cid, S. Cazin, A. Sevrain, H. Djeridi, G. Harran, F. Moradei, GLOBAL MODES AND NEAR WAKE UNSTEADINESS IN THE TURBULENT FLOW AROUND A CIRCULAR CYLINDER AT HIGH REYNOLDS NUMBER BY PIV, (2005).

[17] M. Nili-Ahmadabadi, O. Nematollahi, M. Fatehi, D.S. Cho, K.C. Kim, Evaluation of aerodynamic performance enhancement of Risø_B1 airfoil with an optimized cavity by PIV measurement, J. Vis. 23 (2020) 591–603. https://doi.org/10.1007/s12650-020-00658-7.

[18] H.F. Leite, L.I. de Abreu, D. Schuch, A.C. Avelar, POD AND SPECTRAL ANALYSIS OF A WALL-MOUNTED SQUARE CYLINDER WAKE, (2016).

[19] N. Ertürk, A. Vernet, J. Pallares, R. Castilla, G. Raush, Small-scale characteristics and turbulent statistics of the flow in an external gear pump by time-resolved PIV, Flow Meas. Instrum. 29 (2013) 52–60. https://doi.org/10.1016/j.flowmeasinst.2012.09.004.

[20] Y. Zhong, H. Ma, H. Li, Z. Wang, Q. Li, Influence of surface suction on wake characteristics behind a circular cylinder, J. Vis. (2022). https://doi.org/10.1007/s12650-022-00826-x.

[21] Z. Zhang, C. Ji, D. Xu, Temporal and spatial evolution of vortex shedding for flow around a cylinder close to a wall, Ocean Eng. 228 (2021) 108964. https://doi.org/10.1016/j.oceaneng.2021.108964.

[22] H. Yu, W.-L. Chen, Y. Huang, H. Meng, D. Gao, Dynamic wake of a square cylinder controlled with steady jet positioned at the rear stagnation point, Ocean Eng. 233 (2021) 109157. https://doi.org/10.1016/j.oceaneng.2021.109157.

[23] P.J. Schmid, Dynamic mode decomposition of numerical and experimental data, J. Fluid Mech. 656 (2010)

5–28. https://doi.org/10.1017/S0022112010001217.

[24] T. Sayadi, P.J. Schmid, F. Richecoeur, D. Durox, Parametrized data-driven decomposition for bifurcation analysis, with application to thermo-acoustically unstable systems, Phys. Fluids. 27 (2015) 037102. https://doi.org/10.1063/1.4913868.

[25] H. Ping, H. Zhu, K. Zhang, D. Zhou, Y. Bao, Y. Xu, Z. Han, Dynamic mode decomposition based analysis of flow past a transversely oscillating cylinder, Phys. Fluids. 33 (2021) 033604. https://doi.org/10.1063/5.0042391.

[26] B.-F. Ma, S.-L. Yin, Vortex Oscillations Around a Hemisphere-Cylinder Body with a High Fineness Ratio, AIAA J. 56 (2018) 1402–1420. https://doi.org/10.2514/1.J056047.

[27] B. Jayaraman, C. Lu, J. Whitman, G. Chowdhary, Sparse feature map-based Markov models for nonlinear fluid flows, Comput. Fluids. 191 (2019) 104252. https://doi.org/10.1016/j.compfluid.2019.104252.

[28] M.S. Hemati, M.O. Williams, C.W. Rowley, Dynamic mode decomposition for large and streaming datasets, Phys. Fluids. 26 (2014) 111701. https://doi.org/10.1063/1.4901016.

[29] M. Fathi, A. Bakhshinejad, A. Baghaie, R. D'Souza, Dynamic Denoising and Gappy Data Reconstruction Based on Dynamic Mode Decomposition and Discrete Cosine Transform, Appl. Sci. 8 (2018) 1515. https://doi.org/10.3390/app8091515.

[30] Y. Zhong, H. Ma, D. Yun, J. Guo, B. Xu, Effects of different suction angles on flow structures and dissipation in the wake of a circular cylinder, Ocean Eng. 266 (2022) 112521. https://doi.org/10.1016/j.oceaneng.2022.112521.

[31] W. Yang, Y. Huang, D. Gao, W. Chen, Ludwig Prandtl's envisage: elimination of von Kármán vortex street with boundary-layer suction, J. Vis. 24 (2021) 237–250. https://doi.org/10.1007/s12650-020-00708-0.

[32] Y.Z. Liu, L.L. Shi, J. Yu, TR-PIV measurement of the wake behind a grooved cylinder at low Reynolds number, J. Fluids Struct. 27 (2011) 394–407. https://doi.org/10.1016/j.jfluidstructs.2010.11.013.

[33] G. Tissot, L. Cordier, N. Benard, B.R. Noack, Model reduction using Dynamic Mode Decomposition, Comptes Rendus Mécanique. 342 (2014) 410–416. https://doi.org/10.1016/j.crme.2013.12.011.

[34] J.E. Higham, A. Vaidheeswaran, W. Brevis, F.C.G.A. Nicolleau, J. Marlow, Modification of modal characteristics in wakes of square cylinders with multi-scale porosity, Phys. Fluids. 33 (2021) 045117. https://doi.org/10.1063/5.0049528.

[35] M.A. Mendez, M. Balabane, J.-M. Buchlin, Multi-scale proper orthogonal decomposition of complex fluid flows, J. Fluid Mech. 870 (2019) 988–1036. https://doi.org/10.1017/jfm.2019.212.

[36] M.A. Mendez, D. Hess, B.B. Watz, J.-M. Buchlin, Multiscale proper orthogonal decomposition (mPOD) of TR-PIV data—a case study on stationary and transient cylinder wake flows, Meas. Sci. Technol. 31 (2020) 094014. https://doi.org/10.1088/1361-6501/ab82be.

[37] R. Perrin, M. Braza, E. Cid, S. Cazin, F. Moradei, A. Barthet, A. Sevrain, Y. Hoarau, Near-Wake Turbulence Properties in the High Reynolds Number Incompressible Flow Around a Circular Cylinder Measured by Two- and Three-Component PIV, Flow Turbul. Combust. 77 (2006) 185–204. https://doi.org/10.1007/s10494-006-9043-5.

[38] J.G. Chen, Y. Zhou, R.A. Antonia, T.M. Zhou, Characteristics of the turbulent energy dissipation rate in a cylinder wake, J. Fluid Mech. 835 (2018) 271–300. https://doi.org/10.1017/jfm.2017.765.

[39] H. Jiang, X. Hu, L. Cheng, T. Zhou, Direct numerical simulation of the turbulent kinetic energy and energy dissipation rate in a cylinder wake, J. Fluid Mech. 946 (2022) A11. https://doi.org/10.1017/jfm.2022.587.